TEAM Flexion:

Inductive Charging Station Integrated with the Armadas Voxels

Student Team Members:

Matthew Loi, William Dortch, Jonathan Sanchez, Kin Tsang

Advisor:

Dr. Micheal Thorburn

Mentor:

Horace Lee, Antonella S. Pinola

C3 Cosmic Capstone Challenge 2025-2026

Table of Contents

1.0 - Introduction

1.1 - Background/Problem

The NASA Artemis Program aims to establish a permanent human presence at the Lunar South Pole by utilizing **In-Situ Resource Utilization (ISRU)** to extract water ice for fuel and life support. However, current mission architectures are hindered by a lack of robust power infrastructure. NASA identifies lunar microgrids as essential for extending "daylight" operations and supporting science payloads that lack independent power generation [1].

The **VIPER Exploration Rover** exemplifies these limitations: with a 450 W peak draw, it provides only 9 hours of active operation per charge [2]. To avoid total power failure during eclipse periods or when entering **Permanently Shadowed Regions (PSRs)**, rovers must constantly retreat to high-altitude **Peaks of Eternal Light (PELs)**. This dependence on sporadic sunlight—caused by the Moon's 1.5° axial tilt—results in significant operational downtime and prevents sustained exploration of resource-rich crater floors.

Beyond lighting, the lunar regolith presents a critical mechanical and electrical challenge. The majority of jagged, electrostatically charged dust particles accumulate between **1–5 meters** above the surface due to anthropogenic ejecta and electrostatic levitation [3]. This accumulation makes traditional physical charging connectors (plugs) major points of failure due to abrasive wear and increased electrical resistance. Consequently, a viable lunar microgrid must implement a charging and generation system capable of surviving these extreme lighting contrasts and mitigating the pervasive risks of regolith interference.

1.2 - Project Objective

The objective of this project is to design and outline the assembly process of a charging station for charging exploration rovers at mission critical sites such as ISRU Excavation and Exploration sites. Utilizing the ARMADAS Voxel as a scalable building block and Robotic Assemblers, SOLL-E and MMIC to establish infrastructure that can generate its own power and deliver power wirelessly to exploration rovers operating in PSR regions such as the bottom of the

Shackleton Crater. Structure will be designed to minimize lunar dust accumulation and maximize solar energy generation.

Within the structure will be our charging station which would have approximately 490 W of instantaneous power on standby for the rover. The power will be transferred through an inductive resonance circuit at a high frequency of 160 kHz.

1.3 - Operational Benefit

The proposed charging infrastructure would help to expand the operational time of exploration rovers well into periods of darkness by constantly supplying power from the battery, which stores the captured energy for the period of darkness. In a general lunar cycle of 29.5 days where half of the time we get darkness, the operational timeline could be mapped out as:

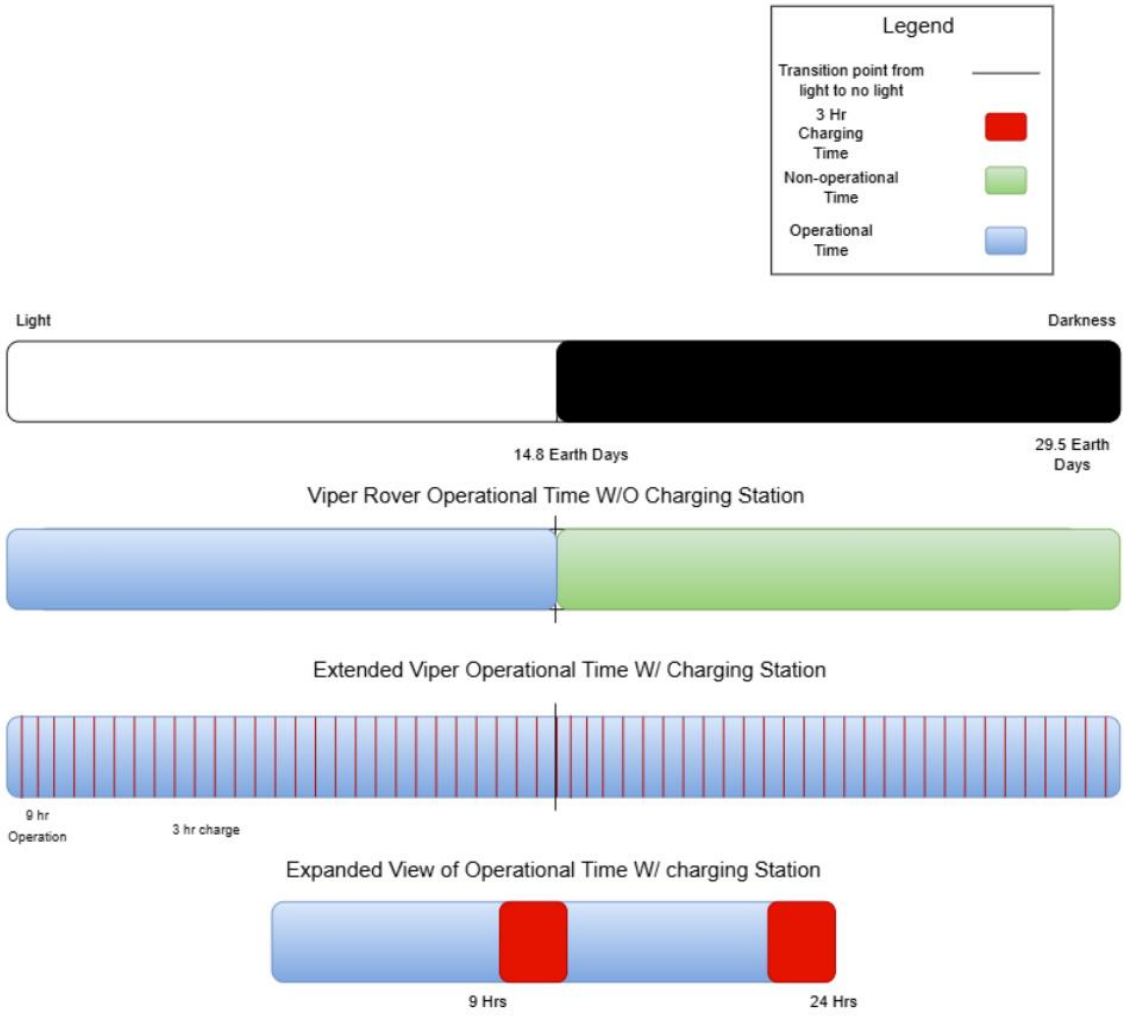

Figure 1. Operational Timeline Comparison

As seen in figure 1, during periods of light the viper is able to perform its mission operations but once we enter the darkness period, the viper effectively goes offline and just travels to different regions collecting the last bit of light until it enters hibernation and waits for light to return as shown in green. With the proposed charging infrastructure, the viper can perform its operations regardless of available solar energy. The only operational downtime the rover experiences is for its 3-hour recharge period which ultimately leads to a 50% increase in operational uptime.

2.0 - System Design Overview

2.1 - Requirements

Location plays a major role in understanding exactly how much solar energy there is available. At the Shackleton Crater, there is a Peak of Eternal Light (PEL) at the rim of the crater located at (89.68°S 166.0°W) which experiences a darkness period of 7 days at the most.

System requirements as shown in Table 1 were defined and developed based on environmental factors, exploration rover energy demand, lunar south pole cycle, and location lighting conditions.

Table 1. Charging Station Requirements

Requirement	Design Specification
Energy Storage Capacity	80 kWh
Total Energy Generated	260 kWh
Average Power Output	481.48 W
Solar Tower Height	> 5m (≈ 16.4 ft)
Thermal Tolerance	System should function in (-232°C to +120°C) [4]

2.2 - Architecture Overview (Electrical and Mechanical)

Mechanical Architecture Overview

The mechanical design is engineered to ensure the survival and long-term operation of the wireless charging station in harsh conditions. The primary focus is on thermal management and material selection.

2.2.1 Thermal Management System

Maintaining the battery within its optimal operating temperature range is crucial for the functionality and purpose of the objective. It is placed in Permanent Shadowed Regions (PSRs). The thermal management system will consist of passive and active elements to maintain operating temperatures.

Passive Thermal Management (Insulation)

Passive management reduces heat loss generated by the battery, minimizing the power required for heating. To retain the heat generated in extreme cold temperatures, an enclosure is required with low thermal conductivity that can maintain structural integrity.

Table 2: Insulation Properties

Insulation Enclosures (material) Study	**Aerogel**	**Polyimide(Kapton)**	**Mica**
Primary Type	Nano-Porous	High -Performance Polymer	paper composed of flakes of muscovite mica
Thermal Conductivity (W/m*K)	0.013	0.12	0.2
Structural Integrity	Extremely Fragile and Brittle	Excellent	Poor

The selected approach is a composite of aerogel and polyimide. This solution takes advantage of aerogel's lowest thermal conductivity, while the polyimide provides the necessary structural integrity [8]. This approach solves the concern about aerogels being fragile and brittle for a lunar environment [6].

Active Thermal Management

Active components regulate temperature to prevent hotspots during charge and discharge cycles.

Table 3: Active Thermal Management Components

Active Thermal Management Options	Purpose	Efficiency (COP, Energy consumption, and Practicality)	Complexity/Maintenance	Exclusion
Electric Resistance Heaters	Heat Generation	High-Performance Polymer	Simple unit with minimal maintenance	Selected: Highly efficient heat generator
Heat Pipes	Heat Transport	High	No moving parts, Tube routing, Tight physical contact	Selected: Can be used to prevent hotspots, transports heat effectively
Liquid Circulator	Bulk Heat Rejection/Cooling	High	Requires pumps, valves, and a control system. Maintenance is moderate	Selected: Utilized to maintain stable temps and/or to remove bulk heat with other components to prevent overheating

The chosen combination of active thermal management of electric resistance heaters, heat pipes, and a liquid circulator is due to low energy consumption and the ability to generate, transport, and reject heat efficiently [9,10,11]

2.2.2 Cable and Wiring Material Selection

The mechanical properties of the cable conductor and the insulation material are for a 4.25km cable between the solar structure and the charging station. There will need to be insulation to withstand the abrasive terrain along the journey.

Conductor Selection

The design prioritizes electrical performance and durability during deployment.

Table 4: Material Selection for the Cable

Property	Copper	Aluminum	Comparison	Relevance for Cable
Absolute Conductivity	5.98E7 S/m	3.5E7 S/m	Copper is more effective than aluminum.	Copper has a lower power loss than aluminum.
Volume Resistivity (Omega, 20C)	1.72 times 10^(-8)	2.82 times 10^(-8)	Aluminum has a higher resistance than copper.	Aluminum will generate more heat due to resistance
Density (kg/m^3)	8,960	2,700	Copper is noticeably higher than aluminum.	Heavier cable may lead to difficulty carrying
Tensile Strength (MPa)	~220	~150	Tensile Strength: Copper is stronger	Higher strength, less prone to breaking
Coefficient of Thermal Expansion (m* C)	16.5	23	Aluminum has a higher expansion	Lower expansion minimizes stress on cables from extreme temperature cycles over time.
Melting Point (C)	1,085	660	Copper has a higher thermal resilience	Copper, having a higher melting point, provides higher tolerance for hot spots or overloads

Copper was selected due to its ability to withstand temperature cycles, higher tensile strength, and lower resistivity, ensuring high reliability for power transmission over long distances.

Insulation Selection

Materials must withstand extreme temperatures, radiation, and abrasive lunar regolith.

Table 5: Insulation Choices for Cable

Property	Polyimide	PTFE/FEP	ETFE
Temperature Ranges	-269°C and 400°C	-200°C to +260°C	-100°C to +150°C
Radiation Resistance	Fair	Poor	Great
Abrasion Resistance	Fair	Good	Excellent

The design takes advantage of a composite of polyimide and ETFE. This takes advantage of polyimide's thermal performance alongside ETFE's superior resistance to radiation and abrasion. It helps mitigate the section of the cable exposed to the sun's elements on the surface [12].

Electrical Architecture Overview

Understanding the electrical aspect of the charging station, it is important to start with how the charging station stores its energy. Lithium-ion, Solid-State, Lithium Sulfur, and Sodium Ion are among the most common types of battery cells being developed or currently being used for space applications. Choosing the right battery material for space application heavily depends on:

1. Energy Density: How much energy you get per kg of weight.
2. Cycle Life: How many times can you recharge and discharge.
3. Efficiency
4. Operating Temperature

Performance	Lithium Ion	Solid State Battery	Lithium Sulfur	Sodium Ion
Energy Density (Wh/kg)	180 - 280	400 - 600	350 - 500	120 - 180
Volume Density (Wh/L)	350 - 550	400 - 800	350 - 700	250 - 400
Cycle Life	~ 5000	5000 - 10000	500 - 1000	1000 - 5000

Round-trip efficiency	90-95%	>90% (Some sources suggest up to 98%)	85 - 95%	90 - 95%
Operating Temp (Celsius)	-20 - +60	-40 - +120 (could operate as low as -60)	-40 - +60	-30 - +80
Lifespan	5 - 15 years	10 - 20 years	5 - 10 years	5 - 15 years

Table 6. Battery Material Comparison

Lithium Ion is currently being used for space exploration, however from the case study, solid state offers better specifications across numerous important criteria such as having the highest energy density, lifespan, and cycle-life, allowing it to be used for longer with less battery degradation overtime. This makes it the ideal choice for space-based application in the future.

Most rovers rely on solar panels or nuclear sources, both of which ultimately rely on direct current (DC) for onboard systems. For our inductive charging approach, the station must convert stored DC power from the solid-state battery to alternating current (AC) using a magnetic resonance circuit. This AC power is transmitted wirelessly through an inductive coil on the charging station and received by a corresponding coil on the rover. Once received, the AC power is rectified back into DC to charge the rovers battery efficiently. This bidirectional conversion ensures compatibility with rover power requirements while enabling reliable wireless energy transfer in a dust-prone environment.

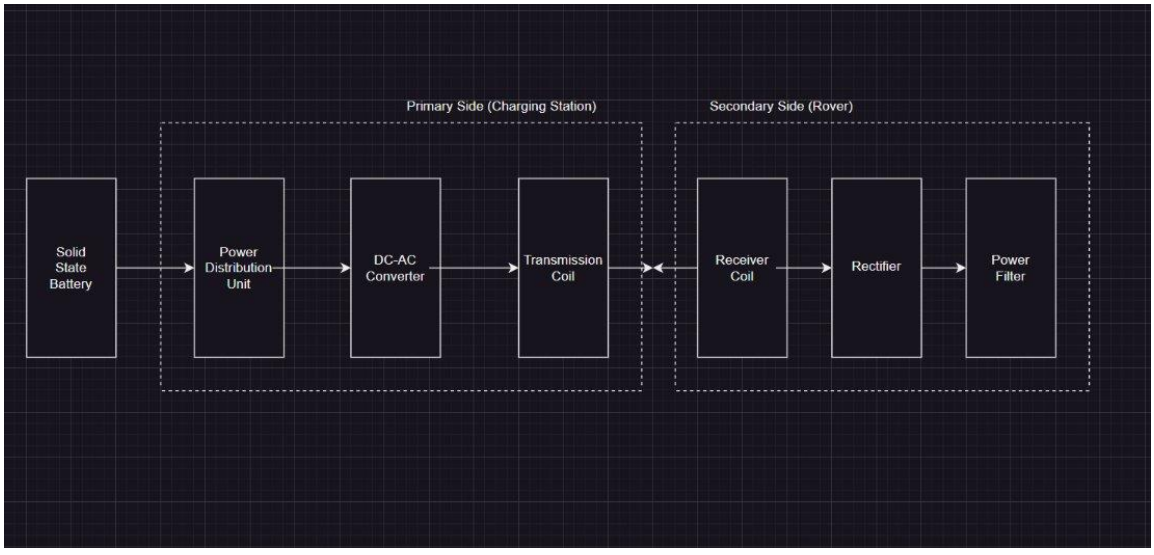

This simple diagram provides a brief description of the major components of the system for the entire charging system. As the power is transferred through AC, the power is rectified to closely get a small amount of ripple where we could assume our magnetic resonance circuit acts similarly to a transformer. The amount of ripple is calculated by $V_{pp} = \frac{I}{2 \cdot f \cdot C}$, if the ripple voltage is low, it could be converted to DC power with high efficiency (Given *I (Current), f (Frequency), C (Capacitance))*. Primary side is considered our charging system which is broken up into solid-state battery, power distribution unit, power filter, and transmission coil. Below is the intended purpose of each component in the charging system.

- Solid-State Battery
    - The energy density of the battery would be around 600 Wh/kg allowing for the battery to be around the mass of 133.33 kg.
    - Alongside the Solid-state battery it will be hooked up to Z4J+ solar panels with 31% power efficiency
- Power Distribution Unit
    - Circuit Protection
        - Given high current will be held and transferred with our charging stations. Creating a protection circuit to manage these high currents will prevent overheating and increase efficiency.
        - Components for Current Protection --> (Fuses, Circuit Breaker, Relay)
    - Current Sensing
        - Controlling the flow of current and changing frequency dependent on the rover's architecture when charging.
        - Overcurrent Detection circuit
    - Proximity Sensor + Buck Converter
        - Using an Ultrasonic or Camera to track distance from the rover to the charging station.
- DC-AC Converter
    - Using MOSFETs to switch constant turning AC waveform to DC.
    - Using a high-functional AC-DC Converter module

Transmission and Receiver Coil Materials

Material Type	Sat Flux Density (T)	Initial Perm.	Frequency
Mn-Zn Ferrite	0.38 - 0.56	$1x10^3$ - $1x10^4$	~100kHz
Ni-Zn	0.25-0.51	$1x10^2$ - $2.3x10^3$	~1 MHz
Ferrite	0.20-0.51	$1.6x10^2$ - $1.3x10^4$	~100kHz-2MHz
Copper	0.01	1	~10MHz
Silver-Plated-Copper	0.01	1	~20MHz
YBCO	0.01	1	~10kHz-5 MHz
Magnetic Alloy	1.2-1.3	$8x10^3$ - $1x10^5$	~1kHz - 500kHz

Table 7. Coil Materials

Selecting coil material is critical for optimizing the efficiency of the magnetic resonance circuit. Conductive materials such as copper, silver-plated copper, and YBCO (high-temp super-conductor) do not inherently have magnetic properties but could generate a magnetic field when current flows through them, thus enabling inductive power transfer. In comparison, materials with intrinsic magnetic properties such as Mn-Zn Ferrite, Ni-Zn Ferrite, and Magnetic Alloys offer high permeability and saturation flux density, which can significantly improve inductive coupling efficiency. These magnetic materials reduce core losses and enhance the magnetic field concentration, making them ideal for core or structural components of the transmission and receiver coils. Combining high-conductivity conductors with high-permeability magnetic cores ensures minimal resistive losses and maximum energy transfer efficiency.

3.0 - Assembly Overview

Pursuant to the requirements of Track 4 in the C3 Challenge, the structure must be comprised of modular building blocks and be built autonomously. The requirement will be proved to be fulfilled through a brief overview of the elements and steps which go towards assembling the tower.

3.1 - ARMADAS Voxel

The Ames Automated Reconfigurable Mission Adaptive Digital Assembly System (ARMADAS) voxel is a modular building block proposed by NASA. The voxel is hollow and is made with carbon fiber reinforced polymer (StattechNN-40CF). The ARMADAS voxel is proposed to have the ability to deliver materials through the pillars on the voxel. For securement, the voxel has 4 captive screws on the corners of the cuboctahedron.

3.2 - SOLL-E, MMIC-I

The ARMADAS voxel are to be made into structures using the robots Scaling Omnidirectional Lattice Locomoting Explorer (SOLL-E) and Mobile Metamaterial Internal Co-Integrator (MMIC-I). The SOLL-E is wishbone-shaped and travels on top of voxels. It features an additional grip on one of the sides of the wishbone which allows the robot to pick up and move voxels. The MMIC-I is a wormlike robot which travels between the voxels to secure two voxels together by engaging the captive screws.

The two robots are powered by ESP32 MCUs which feature wireless protocols on both 2.4Ghz and 5Ghz bands such as Bluetooth and 802.11ac. Due to the preference for using minimal wires, sections of the robot communicate to each other over wireless communication. Data shared include absolute location of each arm of the SOLL-E robot and power states.

3.3 - Build Process

The build process begins by conversion of a structure's voxel locations to WKT code. Then a routing algorithm is applied to the WKT code and processed onboard either an agent or onboard the SOLL-E in a way that allows the building of the structure.

4.0 - Design

4.1 - Design

Category	Component/Option	Key Specification/Value	Structural Rationale
Structure Geometry	Tower Footprint	3ft x 4ft	Consists of 4 corner pillars separated by a 1 ft gap.
Structure Geometry	Total Height	24ft (20 ft pillar + 4 ft array fixture)	
Material Specs	Solar Panel Density	3.3kg/m2 (Astrolab)	[5]
Material Specs	Voxel Unit Mass (Est.)	0.38 kg/voxel	[6]

Table 13. Weight Distribution

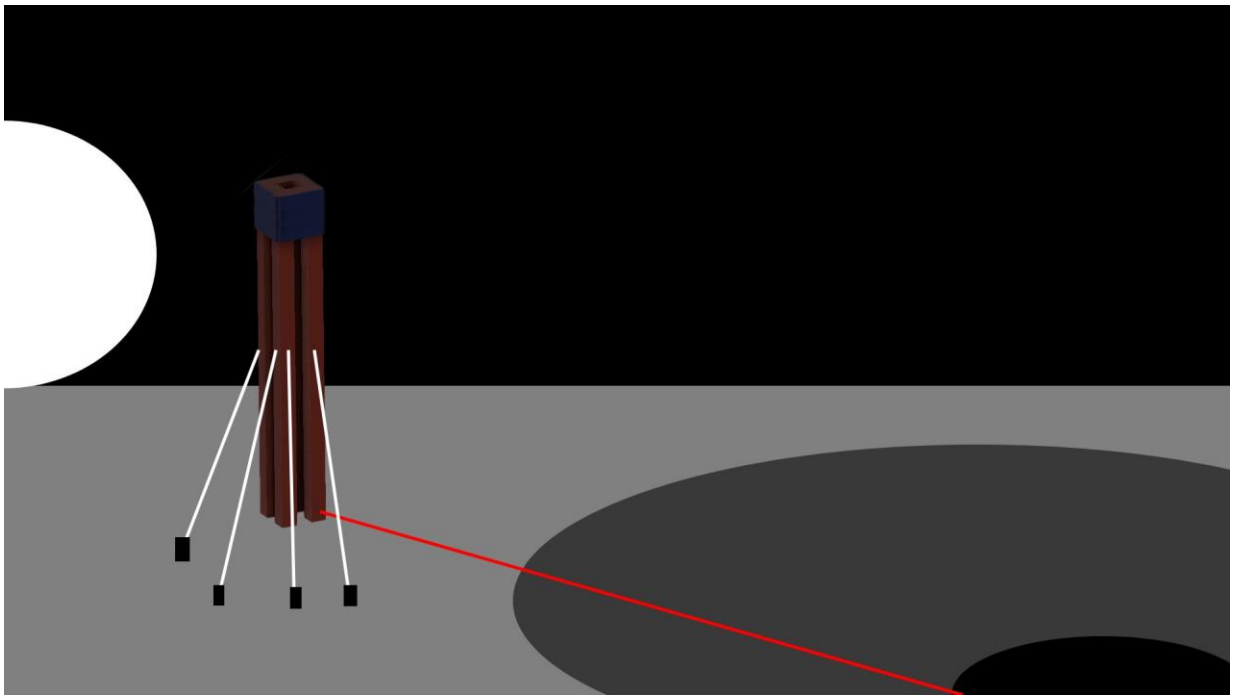

Figure 7. Final Solar Tower Concept Design

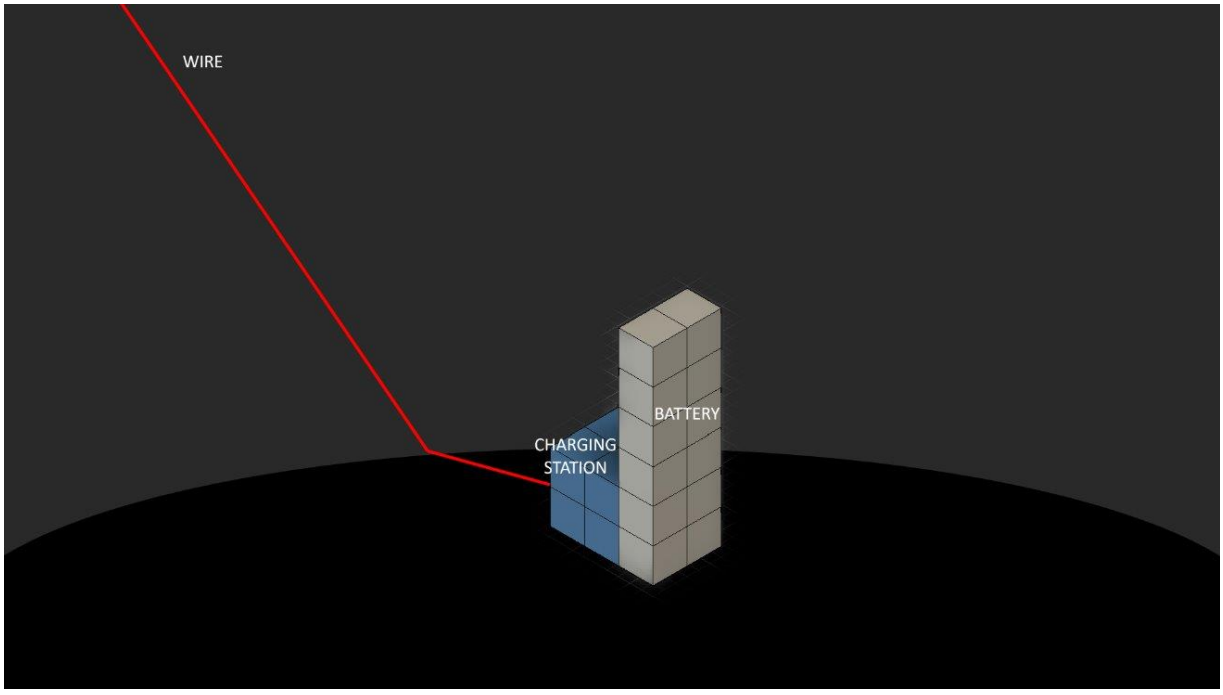

Figure 8. Charging Station Concept Design

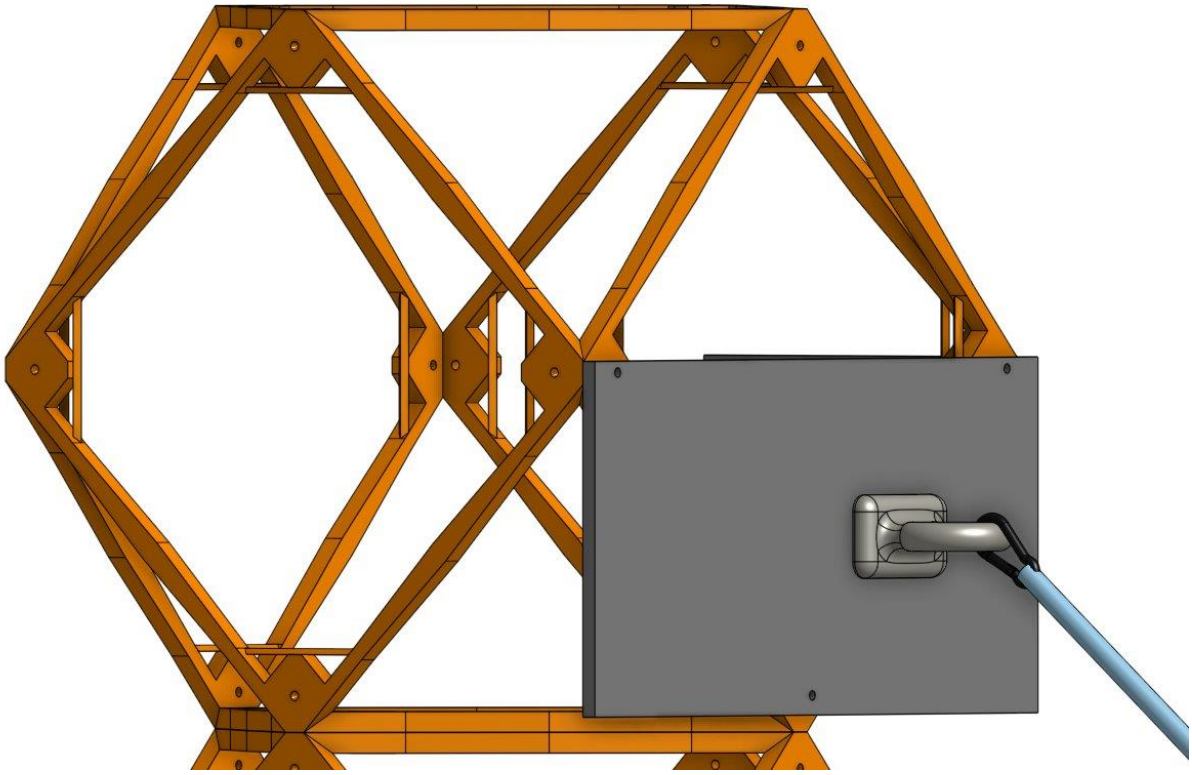

Figure x. Guy Wire CAD Design

An adapter plate for the guy wire gets bolted to the voxel where one end of the guy wire featuring a carabiner gets hooked onto the available hook of the plate.

Charging Methods for Rover				
Method	**AC Type 2**	**DC Fast**	**Inductive**	**V2G**
Explanation	This is a 208 - 240V single or three phase charger which has a average power output of 12.65	This method has a average voltage of 700V DC operating with an average power of 200 kW. This has a charging time of	Inductive power uses inductive resonance coupling which has a 500W power output. This has a charging time on	V2G is a vehicle to grid charging system which has a bidirectional DC or AC interface. This operates around 15kW for a time

	kW for an avg of 5.5 hours	around 15-45 minutes	average around 3.5 hours	around 5.5 hours as well
Complex (30%)	2.25	2.55	2.1	2.1
Durability (25%)	1.5	1.625	2.25	1.25
Efficient (45%)	3.15	3.375	3.825	2.925
Results (100%)	69%	75%	81%	62%

Table 14.Charging Methods

To determine the most suitable approach for our lunar charging station, it is essential to understand the characteristics of each charging method:

- AC Type 2: This is a contact-based charging method where the rover connects to an AC power source. The rover must include an onboard AC-to-DC converter to rectify the alternating current into direct current for battery charging. This approach is common in terrestrial electric vehicles but introduces complexity in dusty lunar environments due to physical connectors.
- DC Fast Charging: Another contact-based method, DC Fast Charging converts AC power to DC within the charging station itself. The station then supplies high-voltage DC directly to the rover, enabling rapid energy transfer. While efficient, this method also relies on physical connectors, which are vulnerable to lunar dust contamination and mechanical wear.
- Vehicle-to-Grid: A bidirectional charging strategy that allows the rover to act as an energy storage device. Using either AC Type 2 or DC Fast interfaces, V2G enables power flow both to and from the grid. While the same limitations of contact-based systems

- Inductive Resonance Charging: This method uses inductive field coupling to transfer power wirelessly, By oscillating a electromagnetic field (induction) at a high frequency, energy is transmitted from stations coil to the rover's coil without physical contact. This eliminates dust-related failures and allows charging at close proximity without precise alignment. Although inductive systems typically deliver lower power compared to DC Fast, they offer superior reliability in harsh lunar conditions.

Our chosen method is Inductive Resonance Charging because it provides a dust-resistant, contactless solution that supports efficient energy transfer within short-range proximity which is ideal for the lunar environment where reliability and reduced maintenance are critical.

5.0 Analysis and Scaling

5.1 - Power and Energy Analysis

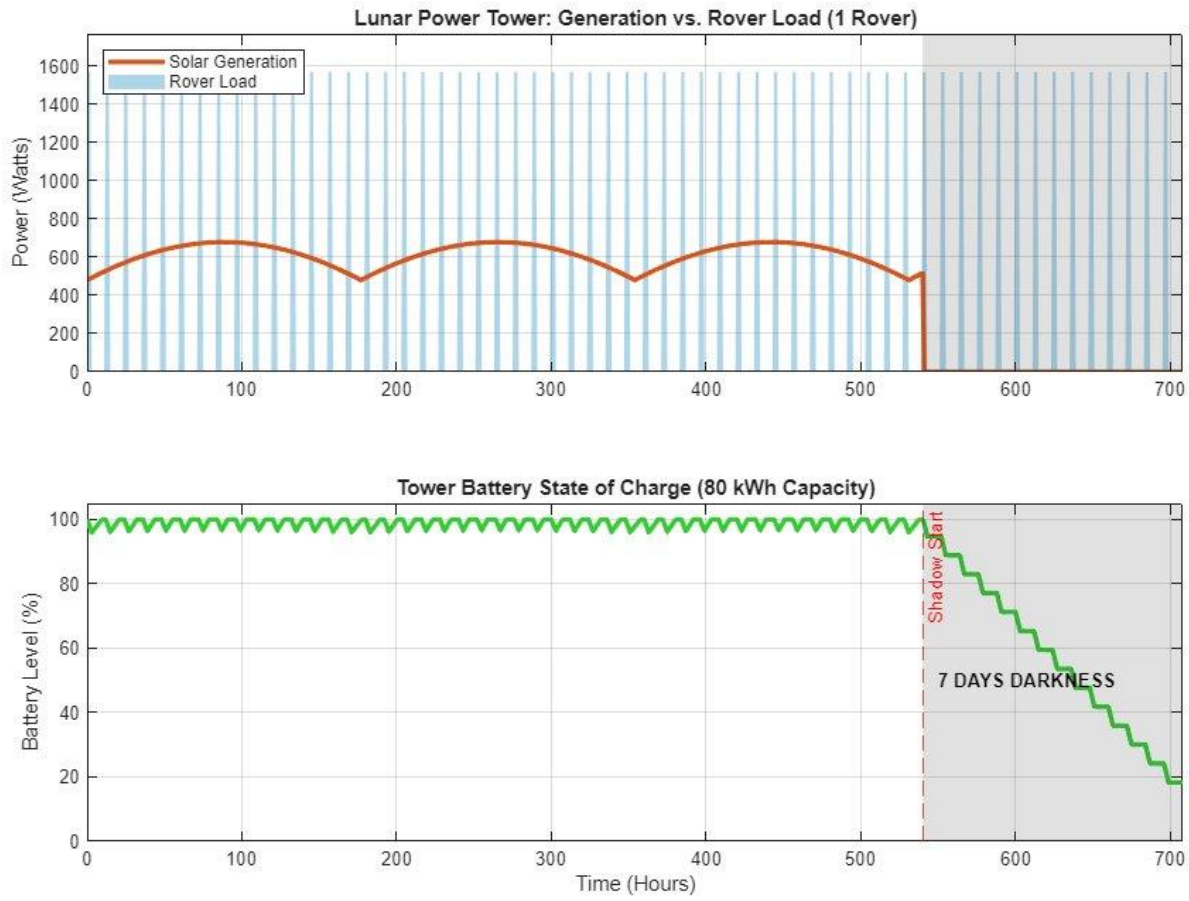

Figure x. Power Generation and Battery S.O.C Simulation

The simulation demonstrates that the Lunar Power Tower effectively manages a high-demand load despite a fluctuating solar input between **480W and 680W**. During the illumination phase (0–540 hours), the system maintains a near-full **State of Charge (SoC)**, with the battery successfully buffering the periodic **1.5kW+ rover spikes** that exceed instantaneous solar generation. The "sawtooth" pattern in the SoC plot confirms a stable charge-discharge cycle, ensuring the **80-kWh battery** enters the lunar night with maximum energy reserves.

Upon the onset of the **7-day shadow period**, the tower transitions to a steady depletion phase, with the SoC stepping down as it supports continued rover loads without solar replenishment. At

the conclusion of the 160-hour darkness cycle, the battery retains approximately **18-20% capacity**. This confirms that the 80-kWh system is appropriately sized for the mission profile, providing a critical power margin to sustain exploration in **Permanently Shadowed Regions (PSRs)** while preventing deep discharge failure.

5.2 - Scaling

To scale this infrastructure for x number of rovers, the system must adhere to specific growth ratios to maintain power stability and operational redundancy. The following scaling laws define the minimum hardware expansion required per additional rover:

1. Increasing battery size by 80 kwh for every additional rover
2. Increasing Solar Panel area by $12ft^2$ for every additional rover
3. Increase amount of charging stations by 1 for every 2 rovers
4. Tower height shall not exceed base width * 20

Each charging station is capped at a **two-rover maximum**; given the 3-hour charge time, this limit provides the necessary operational buffer to prevent scheduling bottlenecks. Structurally, as the solar array width increases to meet higher power demands, additional support blocks should be used under the solar panels to prevent sagging and a new vertical support column for every 5 **ARMADAS Voxel blocks**. Furthermore, for missions exceeding a single rover, a multi-tower configuration is recommended to distribute power generation across independent structures, ensuring mission-critical redundancy and system reliability through a decentralized microgrid.

6.0 Conclusion

Our design achieves both simplicity and efficiency. By arranging solar panels around the voxel-assembled structure, we enable omnidirectional solar capture, ensuring more consistent power generation to support the charging station. With this improved generation capability, we conducted a trade study to identify the most effective rover charging method for lunar conditions. Physical connections were ruled out due to risks of electrical arcing and high power losses. The most reliable option was inductive wireless charging, implemented through a high-frequency RLC circuit, which avoids mechanical wear and protects sensitive electronics.

7.0 References

[1] J. Csank and G. Thomas, "Microgrids on the Lunar Surface," NASA Glenn Res. Center, Cleveland, OH, USA, Tech. Rep. 20220014598, 2022. [Online]. Available: https://ntrs.nasa.gov/api/citations/20220014598/downloads/OFCC%20Microgrids%20on%20the%20Lunar%20Surface.pdf

[2] "Five Things to Know About NASA's Lunar Rover 'VIPER'," Smithsonian Mag., Oct. 12, 2021. [Online]. Available: https://www.smithsonianmag.com/science-nature/five-things-to-know-about-nasas-lunar-rover-viper-180978787/.

[3] H.-W. Hsu and M. Horányi, "Ballistic motion of dust particles in the Lunar Roving Vehicle dust trails," Amer. J. Phys., vol. 80, no. 5, pp. 452–456, 2012, doi: 10.1119/1.3699957.

[4] F. Cain, "Why Is The Moon's South Pole So Important? It's All About Water," Universe Today, Jul. 2019. [Online]. Available: https://www.universetoday.com/articles/why-is-the-moons-south-pole-so-important-its-all-about-water.

[5] Rocket Lab, "Customizable Solar Array Solutions for Satellites S T A R R A Y," [Online]. Available: https://rocketlabcorp.com/assets/Uploads/RL-SolAero-Data-Sheet-StarRay-final.pdf.

[6] I. W. Park et al., "SOLL-E: A Module Transport and Placement Robot for Autonomous Assembly of Discrete Lattice Structures," in Proc. IEEE/RSJ Int. Conf. Intell. Robots Syst. (IROS), Detroit, MI, USA, 2023, pp. 1-8. [Online]. Available: https://ntrs.nasa.gov/api/citations/20230011353/downloads/IEEE_IROS_2023_SOLLE_Final.pdf

[7] "Discovering the Thermal Conductivity of Aerogel Blankets, Using the Thermtest Heat Flow Meter," Thermtest. [Online]. Available: https://thermtest.com/application/aerogel-thermal-conductivity-hfm#:~:text=Aerogel%20Thermal%20Conductivity%20Results,cryogenic%20or%20heat%20intensive%20environments.

[8] "Polyimide," Massachusetts Institute of Technology - 6.777 Material Properties. [Online]. Available: https://www.mit.edu/~6.777/matprops/polyimide.htm. Accessed: Dec. 5, 2025.

[9] "Space," Advanced Cooling Technologies. [Online]. Available: https://www.1-act.com/industries/space/. Accessed: Dec. 5, 2025.

[10] W. G. Baugh and E. J. Picha, "A review of spacecraft thermal control techniques," NASA, Washington, D.C., Rep. NASA-CR-133549, May 1973.

[11] NASA, "7-soa-thermal-2024," NASA, Washington, D.C., Feb. 2024. [Online]. Available: https://www.nasa.gov/wp-content/uploads/2025/02/7-soa-thermal-2024.pdf.

[12] C. Li and C. Li, "Thermal control materials, systems, and design for spacecraft: A review," *Energy Build.*, vol. 215, Art. no. 109890, May 2020.

[13] Wei, X., Wang, Z., & Dai, H. (2014). A Critical Review of Wireless Power Transfer via Strongly Coupled Magnetic Resonances. *Energies*, *7*(7), 4316–4341. https://doi.org/10.3390/en7074316

[14] Rong, C., Yan, L., Li, L., Li, Y., & Liu, M. (2023). A Review of Metamaterials in Wireless Power Transfer. *Materials*, *16*(17), 6008. https://doi.org/10.3390/ma16176008

[15] C. Gregg *et al.*, "Ultra-light, strong, and self-reprogrammable mechanical metamaterials," *Sci. Robot.*, vol. 9, no. 86, Jan. 2024, Art. no. eadi2746, doi: 10.1126/scirobotics.adi2746.

[16] J. Solle, O. I. B. Formoso, C. Gregg, and K. C. Cheung, "SOLL-E: A Module Transport and Placement Robot for Autonomous Assembly of Discrete Lattice Structures," in *Proc. IEEE/RSJ Int. Conf. Intell. Robots Syst. (IROS)*, Detroit, MI, USA, 2023, pp. 3192–3199, doi: 10.1109/IROS55552.2023.10341513.